9742 *J. Phys. Chem. A* **2008,** *112,* 9742–9750

Reaction of Iminopropadienones with Amines—Formation of Zwitterionic Intermediates, Ketenes, and Ketenimines

Rakesh Naduvile Veedu,[†] Okanya J. Kokas,[†] Isabelle Couturier-Tamburelli,[‡] Rainer Koch,[§] Jean-Pierre Aycard,[‡] Fabien Borget,* and Curt Wentrup[†],*

Chemistry Building, School of Molecular and Microbial Sciences, The University of Queensland, Brisbane, Qld 4072, Australia, Physique des Interactions Ionique et Moléculaire, UMR 6633, Université de Provence et CNRS, Centre de St Jérôme, Case 252, 13397 Marseille cedex 20, France, and Institut für Reine und Angewandte Chemie and Center of Interface Science, Carl von Ossietzky Universität Oldenburg, PO Box 2503, 26111 Oldenburg, Germany

Received: April 17, 2008; Revised Manuscript Received: June 10, 2008

Five aryliminopropadienones **4a−d** have been synthesized by flash vacuum thermolysis (FVT) by using two different precursors in each case. These compounds were deposited at 50 K at a pressure of ca. 10^{-6} mbar together with three different nucleophiles, namely, trimethylamine (TMA), dimethylamine (DMA), and diethylamine (DEA), in order to study their reactions as neat solids during warm-up by FTIR spectroscopy. The reaction with TMA showed that a zwitterionic species (**5** and/or **6**) was formed in all the cases. With DMA and DEA, an α-oxoketenimine and/or an imidoylketene (**7** and **8** or **9** and **10**) was formed as the final product. In addition, several bands were observed, which can be assigned to zwitterionic intermediates (**11** or **12**). Optimized structures and vibrational spectra for all products were calculated at the B3LYP/6-31G(d) level of theory by using the polarizable continuum model ($\varepsilon = 5$).

Introduction

The formation of zwitterionic intermediates has been established in the reactions of carbon suboxide (C_3O_2) with trimethylamine (TMA) and dimethylamine (DMA).[1] This results from the nucleophilic attack of the amine on a C=O group of the cumulene.[2]

We have now examined the reactivity of several C_3O_2 analogues, viz. the iminopropadienones R−N=C=C=C=O. Most iminopropadienones are not stable at room temperature and have only been studied at cryogenic temperatures by using matrix isolation IR spectroscopy.[3] However, some iminopropadienones are isolable at room temperature, and this has allowed the recording of ^{13}C NMR spectra in several cases.[4] They are mostly generated by flash vacuum thermolysis (FVT) from precursors such as 1,3-dioxane-4,6-diones (Meldrum's acid derivatives) and isoxazolopyrimidinone derivatives.[3−5] We have investigated the reactivity of the iminopropadienones with different amines, viz. DMA, diethylamine (DEA), and TMA.

Experimental Section

Synthesis of Precursors. The iminopropadienones **4a−d** were synthesized from two types of precursor, the Meldrum's acid derivatives **1a**, **b**, **d**, **e**, and the isoxazolopyrimidinones[5] **2a−e**. In the case of 2-pyridyliminopropadienone **4c**, the Meldrum's acid derivative is not obtainable, and the chloropyridopyrimidinone[3d] **3** was used as an alternative precursor. The Meldrum's acid precursors were synthesized by the reaction of 5-(bismethylthiomethylene)-2,2-dimethyl-1,3-dioxane-4,6-dione[3a−c,e] with the respective arylamine, viz. aniline,[3a,b] 2,6-difluoroaniline,[5] and 3- and 4-aminopyridines.

SCHEME 1

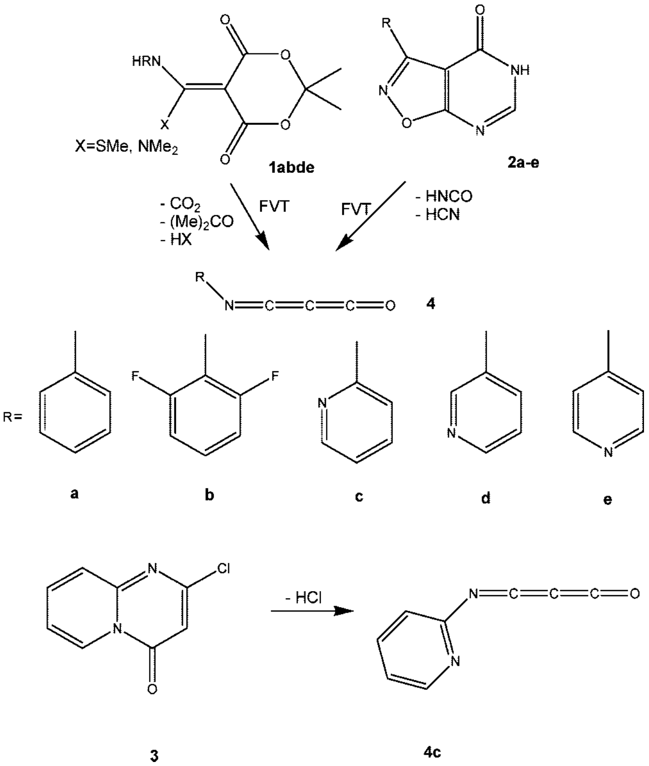

The isoxazolopyrimidinones **2a−e** were synthesized from the corresponding carboxaldehyde by adapting standard protocols.[5−7] Full details of all new compounds are given in the Supporting Information document.

FVT and Matrix Isolation. The iminopropadienones were produced by FVT as described in Scheme 1. The precursors were sublimed at ca. 100 °C and pyrolyzed at 700 °C under a

---

* wentrup@uq.edu.au, fabien.borget@univ-provence.fr.
[†] University of Queensland.
[‡] Université de Provence.
[§] Carl von Ossietzky Universität Oldenburg.

10.1021/jp803351q CCC: $40.75

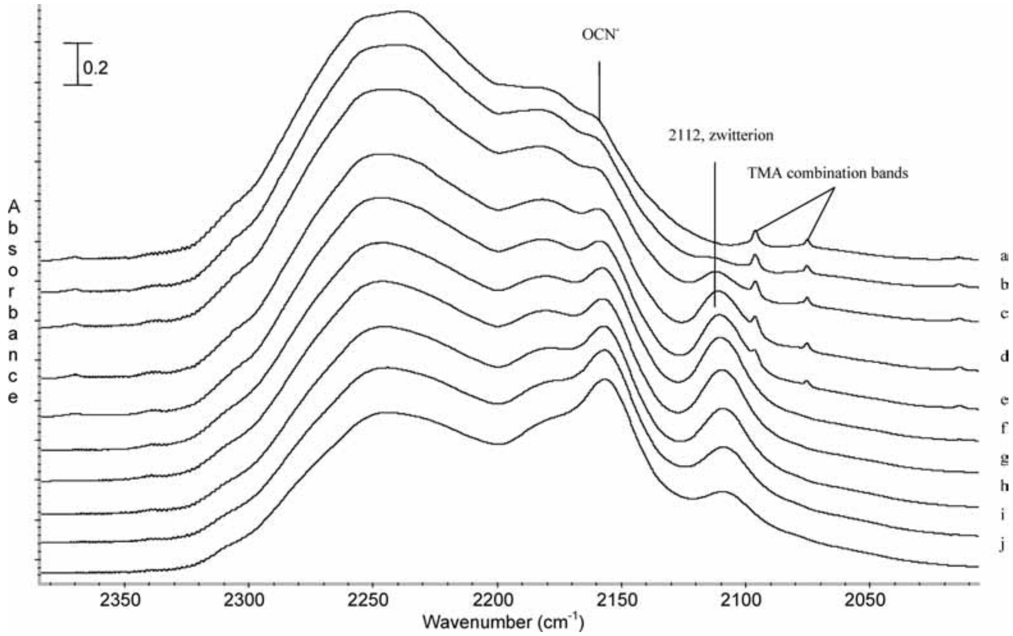

Figure 1. Phenyliminopropadienone (**4a**) from **2a** with TMA deposited at 50 K and recorded at (a) 50 K, (b) 80 K, (c) 90 K, (d) 100 K, (e) 110 K, (f) 120 K, (g) 130 K, (h) 140 K, (i) 150 K, and (j) 160 K.

constant pressure of ca. 10^{-6} mbar to generate the corresponding iminopropadienones. These compounds are not stable enough to be isolable at room temperature. The products of pyrolysis were deposited together with different amines in Ar gas on a CsI window cooled to 50 K in a cryostat at a pressure of ca. 10^{-6} mbar. Each amine, DMA, DEA, and TMA, was previously mixed with Ar in a gas bulb in the ratio 1:350, and this mixture was used as a carrier gas during the FVT reaction. The deposited neat solids comprised mixtures of the pyrolysis products (iminopropadienones and byproducts) and the amine. Because of the low pressure and excess of Ar used, little reaction took place in the gas phase prior to deposition. Because of the deposition temperature of 50 K, Ar was not condensed. After recording the initial IR spectrum, the solid was warmed from 50 to 200 K at a rate of 2 K/min in order to induce mobility of the compounds. The ensuing reactions were monitored by FTIR spectroscopy.

Computational Details

Calculations were performed by using the Gaussian 03 package[8] with the B3LYP[9] density functional method and the 6-31G(d)[10] basis set, together with the PCM SCRF approach.[11] The application of a solvent field is justified by the fact that the reactions investigated herein take place in an amine matrix which certainly stabilizes reactive intermediates. Dielectric constants between 5 and 40 have often been used for the study of related systems.[12] In this paper, we used a dielectric constant of 5, a value close to those of liquid TMA (2.5), DMA (6.3), and DEA (3.7). The exact value of ε has only a minor effect on the appearance of the calculated IR spectra and a negligible effect on the calculated energies.[11] The harmonic frequencies were calculated after geometry optimization at the same level of theory, and all frequencies were scaled by a standard factor of 0.9613.[13]

Results and Discussion

The pyrolysis of the precursors involves the generation not only of the iminopropadienones but also of the byproducts characteristic of each precursor (Scheme 1). Therefore, we first examined the potential reactions of these byproducts with the amines. In the case of the Meldrum's acid derivatives **1**, FVT produces iminopropadienones, CO_2, and acetone (Scheme 1). Acetone did not give any reaction with DMA, DEA, and TMA at the pressure (10^{-6} mbar) and temperatures (50−200 K) used. However, alkylammonium alkylcarbamate ions formed by reaction of CO_2 with the amines can be observed in the spectra; they are characterized by bands growing around 1550, 1400, and 1340 cm^{-1} region[14] (see the Supporting Information). These compounds do not give rise to any bands in the spectral window relevant for the iminopropadienones and the reaction products. In the case of the isoxazolopyrimidinones **2**, HNCO and HCN are produced at the same time as the iminopropadienones (Scheme 1). In contrast to HNCO, the HCN did not show any reactivity. In solid phase, HNCO has strong and characteristic bands at 2252 and 2259 cm^{-1} when it is in an environment of solid NH_3.[15,16] It is well-known that HNCO reacts with NH_3 even at low temperature to produce OCN^-, which is easily identified by a band at 2165 cm^{-1} in solid alkali cyanates or at 2151 cm^{-1} when embedded in solid NH_3.[15,16] Consequently, in all our spectra arising from FVT of isoxazolopyrimidinones, a band appears between 2162 and 2156 cm^{-1} during warm-up of the deposited products. We ascribe this band to OCN^- embedded in a matrix of the amine. A large excess of amines was used in order to examine the iminopropadienone reactivity.

Reaction with TMA. The unsubstituted phenyliminopropadienone **4a** was generated from two different precursors, the Meldrum's acid derivatives **1a** and the isoxazolopyrimidinone **2a**. **4a** was deposited with TMA at 50 K. **4a** is characterized[3] by two bands at 2228 and 2193 cm^{-1} (from **1a**) and at 2237 and 2183 cm^{-1} (from **2a**; see Figure 1). This difference in wavenumbers is probably due to the differences in the matrix environments of each deposited compound. When **2a** was used as a precursor, a band was observed at 2161 cm^{-1} because of the formation of the cyanate anion OCN^- arising from the reaction between HNCO and TMA (see discussion above,[15,16] Figure 1). In Figures 1 and 2, combination bands of TMA are

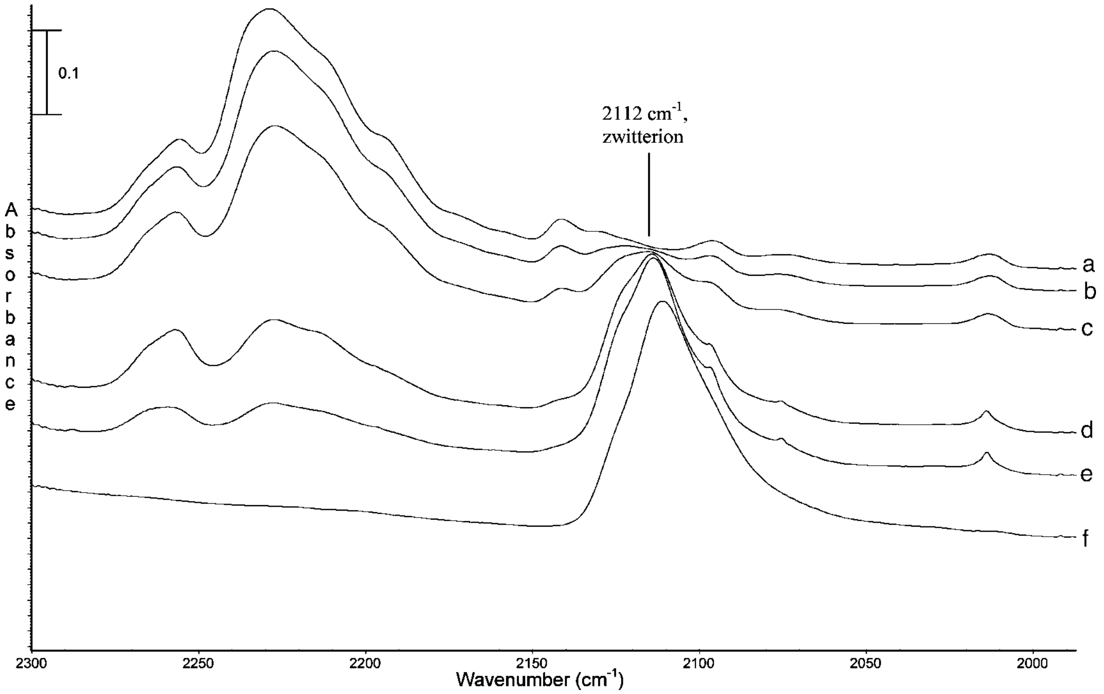

Figure 2. Difluorophenyliminopropadienone from **1b** with TMA deposited at 50 K, then recorded at (a) 50 K, (b) 70 K, (c) 80 K, (d) 90 K, (e) 100 K, and (f) 140 K.

SCHEME 2

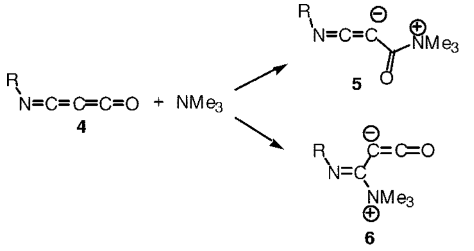

also observable at 2075 and 2095 cm^{-1}. When the temperature was increased, at 80−90 K, a new band grew at 2112 cm^{-1}; at the same time, the bands of **4a** were decreasing. The new band was growing until ca. 110 K and then decreased when the desorption of all the species began. This 2112 cm^{-1} band is ascribed to the formation of a zwitterion **5a** or **6a** (Scheme 2) based on the SCRF calculations.

For each iminopropadienone, two different zwitterions, **5** and **6** (Scheme 2), corresponding to the nucleophilic attack of the TMA (and DMA, compounds **11** and **12**) on the C═O and N═C carbon atoms, were optimized in a simulated solvent field. As shown in Figure 1 and Table 1, the predicted frequencies of the harmonic vibrations allow the assignment of the bands around 2112 cm^{-1} to one of the zwitterions **5** or **6**. In all cases,

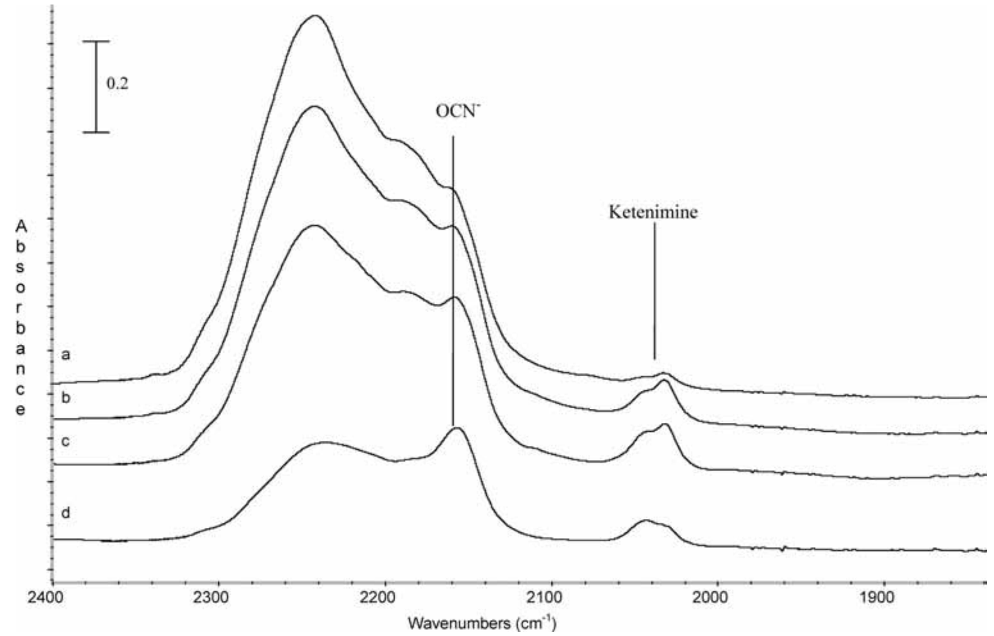

Figure 3. Phenyliminopropadienone (**4a**) from **2a** with DMA deposited at 50 K, then recorded at (a) 100 K, (b) 120 K, (c) 140 K, and (d) 200 K.

TABLE 1: Experimental and Theoretical Main Bands Obtained after Reaction of Iminopropadienones 4 with TMA and DMA[a]

starting iminopropadienone **4**	experimental frequencies (cm^{-1}): iminopropadienone **4**	experimental frequencies (cm^{-1}): species formed in reaction with TMA	intermediate species formed with DMA	theoretical frequencies (cm^{-1}): zwitterions **6** and **12** from nucleophilic attack on C=N	theoretical frequencies (cm^{-1}): zwitterions **5** and **11** from nucleophilic attack on C=O
4a from **1a**	2228 (s)	2112 (s)		2172 (**6a**)	2118 (**5a**)
4a from **2a**	2237 (s)	2112 (s)			
4b from **1b**	2229 (s)	2114 (s)		2116 (**6b**)	2124 (**5b**)
4b from **2b**	2228 (s)	2112 (s)			
4c from **3**	2230 (s)	2116 (m)		2172 (**6c**)	2128 (**5c**)
4c from **2e**	2237 (s)	2117 (s)			
4d from **1d**	2221 (s)	2115 (s)		2171 (**6d**)	2127 (**5d**)
4e from **1e**	2222 (s)	2113 (s)		2144 (**6e**)	2127 (**5e**)
4a from **1a**	2228 (s)		2112 (s)	2150 (**12a**)	2123 (**11a**)
4b from **1b**	2229 (s)		2114 (s)	2097 (**12b**)	2126 (**11b**)
4c from **3**	2230 (s)		2116 (m)	2115 (**12c**)	2127 (**11c**)
4d from **1d**	2221 (s)		2115 (s)	2145 (**12d**)	2125 (**11d**)
4e from **1e**	2222 (s)		2113 (s)	2113 (**12e**)	2128 (**11e**)

[a] Theoretical frequencies with B3LYP/6-31G(d) obtained by using an SCRF method with $\varepsilon = 5$ and a scaling factor of 0.9613. Intensities: s, strong; m, medium; w, weak.

TABLE 2: Experimental and Theoretical Main Bands Obtained after Reaction of Iminopropadienones 4 with DMA[a]

starting iminopropadienone **4**	experimental frequencies (cm^{-1}): iminopropadienone **4**	experimental frequencies (cm^{-1}): species formed in reaction with DMA	theoretical frequencies (cm^{-1}): ketene **8**	theoretical frequencies (cm^{-1}): ketenimine **7**
4a from **1a**	2244 (s)	2032 (m)	2120 (**8a**)	2039 (**7a**)
4a from **2a**	2242 (s)	2033 (m)		
4b from **1b**	2231 (s)	2142 (m),2131 (m)/2039 (m)	2123 (**8b**)	2043 (**7b**)
4b from **2b**	2236 (s)	2144 (s)/2043 (m), 2027 (m)		
4c from **3**	2231 (s)	2124 (s)/2032 (m)	2124 (**8c**)	2047 (**7c**)
4d from **2d**	2226 (s)	2134 (w) /2034 (w)	2124 (**8d**)	2039 (**7d**)
4e from**1e**	2223 (s)	2127 (m)/2033 (w)	2127 (**8e**)	2045 (**7e**)
4e from **2e**	2229 (s)	2130 (m)/2027 (w)		

[a] Theoretical frequencies with B3LYP/6-31G(d) obtained by using an SCRF method with $\varepsilon = 5$ and a scaling factor of 0.9613. Intensities: s, strong; m, medium; w, weak. In the reactions of **4b**−**e** with DMA, two sets of growing bands were observed, indicating that both ketene and ketenimine are formed.

SCHEME 3

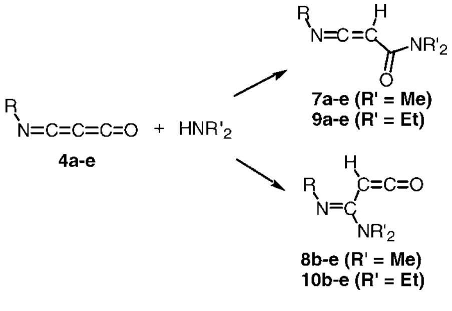

the calculated values for the TMA addition at the C=O end (**5**) are closer to the experimental values, except for **6b**, which possesses a distorted structure and hence gives a smaller value for the C=C=N vibration. Although it is not possible to determine with absolute certainty, these data are a strong indication for the formation of a zwitterion resulting from C=O addition.

The difluorophenyliminopropadienone **4b** was generated from the precursors **1b** and **2b** and deposited with TMA at 50 K. No reaction took place at this temperature. **4b** is characterized[3] by three bands at 2255, 2229, and 2193 cm^{-1} when using **1b** as the precursor (Figure 2) and a broadband centered at 2228 cm^{-1} when using **2b** (see Supporting Information). When the temperature of the matrix was increased to ca. 70 K, a new band appeared at 2114 cm^{-1} (when using **1b** as the precursor) or 2112 cm^{-1} (when using **2b** as the precursor), see Table 1. Intensities of bands due to **4b** decreased at the same time. The 2112−2114 cm^{-1} band was growing until ca. 140 K and then decreased because of desorption of all the species in the matrix. When **2b** was used as precursor, a second band was growing at 2152 cm^{-1}; this is shown in the Supporting Information and is ascribed to the formation of the OCN$^-$ ion formed by reaction between HNCO and TMA.

An analogous experiment was carried out with iminopropadienone **4b** and pyridine. Here, a new band at 2112 cm^{-1} appeared on warming to ca. 70 K. This type of experiment has been performed previously with C_3O_2 and pyridine;[1,17] in the case of the reaction of C_3O_2 with TMA,[1] a zwitterion was clearly observed experimentally between 2129 and 2082 cm^{-1}, and its structure was corroborated by SCRF calculations.

TMA was deposited with all three pyridyliminopropadienones **4c**−**e** at 50 K. The reactions with **4c**, **4d**, and **4e** gave rise to products with characteristic bands at 2117, 2115, and 2113 cm^{-1}, respectively (all the spectra are shown in the Supporting Information). The experimental and calculated frequencies for the zwitterions (**5** or **6**) resulting from reaction of **4a**−**e** are reported in Table 1.

Reaction with DMA and DEA. Iminopropadienone **4a** was deposited with DMA at 50 K. The resulting IR spectrum showed bands belonging to both compounds. **4a** is characterized[3] by two bands at 2244 and 2184 cm^{-1} from precursor **1a** and at 2242 and 2186 cm^{-1} from **2a**. When the temperature was increased to ca. 100 K, a new band started growing at 2032 cm^{-1}, and at the same time, the intensities of bands due to **4a**

TABLE 3: Experimental and Theoretical Main Bands Obtained after Reaction of Iminopropadienones 4 with DEA[a]

	experimental frequencies (cm-1)		theoretical frequencies (cm-1)	
starting iminopropadienone **4**	iminopropadienone **4**	species formed in reaction with DEA	ketene **10**	ketenimine **9**
4a from **1a**	2228 (s)	2109 (w)/2033 (m)	2118 (**10a**)	2039 (**9a**)
4a from **2a**	2235 (s)	2033 (m)		
4b from **2b**	2236 (s)	2143 (w), 2041 (w)	2121 (**10b**)	2042 (**9b**)
4c from **3**	2226 (s)	2126 (s), 2037 (m)/2015 (m)	2122 (**10c**)	2048 (**9c**)
4d from **1d**	2226 (s)	2140 (w)/2116 (m)/2035 (m)	2120 (**10d**)	2038 (**9d**)
4d from **2d**	2224 (s)	2149 (m)/2120 (w)/2028 (m)		
4e from **1e**	2224 (s)	2152 (w)/2113 (w)/2036 (w)	2124 (**10e**)	2045 (**9e**)

[a] Theoretical frequencies with B3LYP/6-31G(d) obtained by using an SCRF method with $\varepsilon = 5$ and a scaling factor of 0.9613. Intensities: s, strong; m, medium; w, weak. In the reactions of **4a**−**e** with DEA, two sets of growing bands were observed, indicating that both ketene and ketenimine are formed. For **4b**−**d**, bands ascribed to zwitterions were also observed (2113−2116 cm^{-1}, see text).

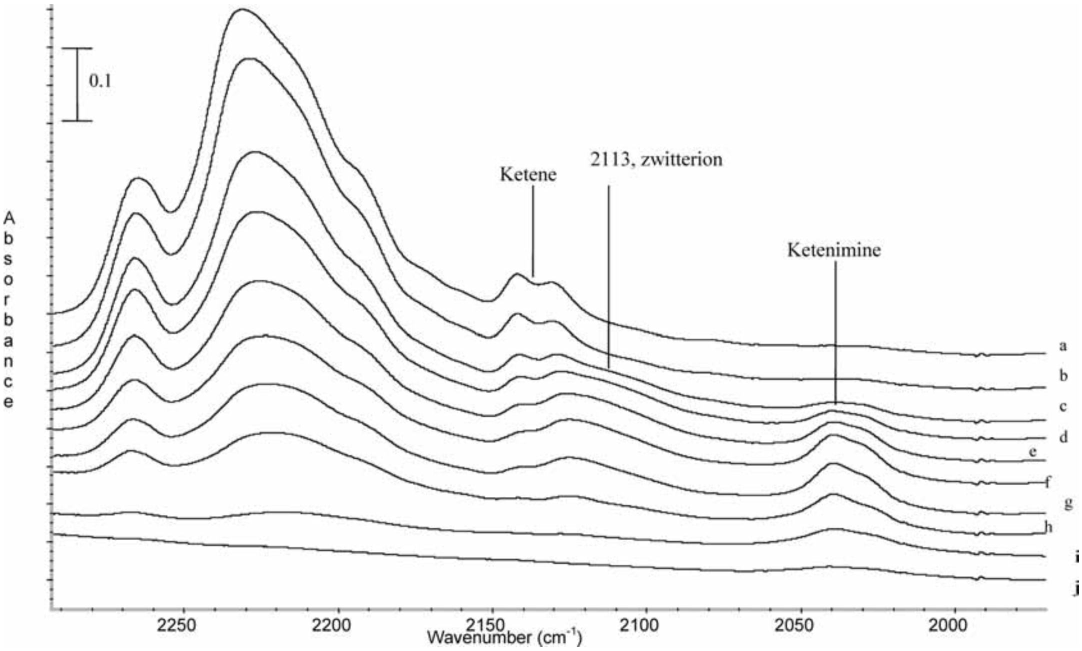

Figure 4. Difluorophenyliminopropadienone (**4b**) from 1b with DEA deposited at 50 K and recorded at (a) 50 K, (b) 80 K, (c) 100 K, (d) 110 K, (e) 120 K, (f) 130 K, (g) 140 K, (h) 150 K, (i) 200 K, and (j) 240 K.

SCHEME 4

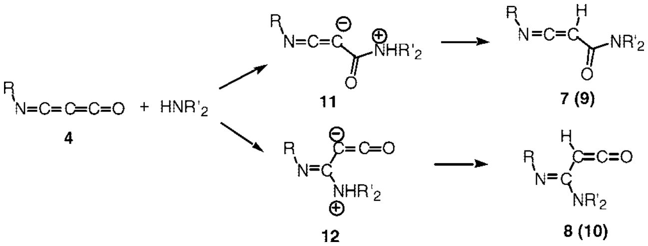

decreased (Figure 3, Table 2). The new peak reached its maximum intensity at 120 K, and it is ascribed to the ketenimine **7a** (Scheme 3) because analogous ketenimines with similar absorptions have been observed.[3,12] During the warm-up, a shift from 2032 to 2042 cm^{-1} is seen, probably due to a phase change.

Compound **4a** was also deposited with DEA at 50 K, giving rise to bands at 2228 and 2193 cm^{-1} when generated from precursor **1a** and at 2235 and 2186 cm^{-1} from **2a**. At 100 K, a new ketenimine band grew in at 2032−2033 cm^{-1} depending on the precursor. This is ascribed to **9a**. The main experimental and calculated bands for the ketenimines **7** and **9** and ketenes **8** and **10** are listed in Tables 2 and 3. The experimental values are in good agreement with the calculated bands and support the formation of ketenimines **7a** and **9a**.

The difluorophenyliminopropadienone[5] **4b** was deposited with DMA by using the same conditions as those reported above for **4a**. Compound **4b** is characterized by a double band at 2264 and 2231 cm^{-1} when formed from the Meldrum's acid derivative **1b** and a broad band at 2236 cm^{-1} when derived from the isoxazolopyrimidinone **2b**. Two other important bands appear between 2156 and 2130 cm^{-1} in all matrices arising from depositions of **4b** and DMA. They are assigned to the ketene **8b**, formed in a gas-phase reaction between **4b** and the amine (see Supporting Information). Moreover, in the spectrum arising from deposition of **4b** (from **2b**) with DEA, analogous bands at 2143 and 2130 cm^{-1} indicate a gas-phase reaction forming ketene **10b** (Figure 4, Scheme 3). It should be noted that the formation of ketene and/or ketenimine in the gas phase has only a bearing on the thermodynamics and not on the kinetics, because it is known that imidoylketenes and α-oxoketenimines of these types interconvert with low energies of activation (≤45−50 kJ/mol).[12c,d] Thus, the present low temperature studies are necessary in order to determine which species are formed first.

Annealing of the matrix containing **4b** and DEA to 100 K caused a new band to grow at 2039 cm^{-1}, and a new shoulder appeared at 2113 cm^{-1} (Figure 4). This latter band continued

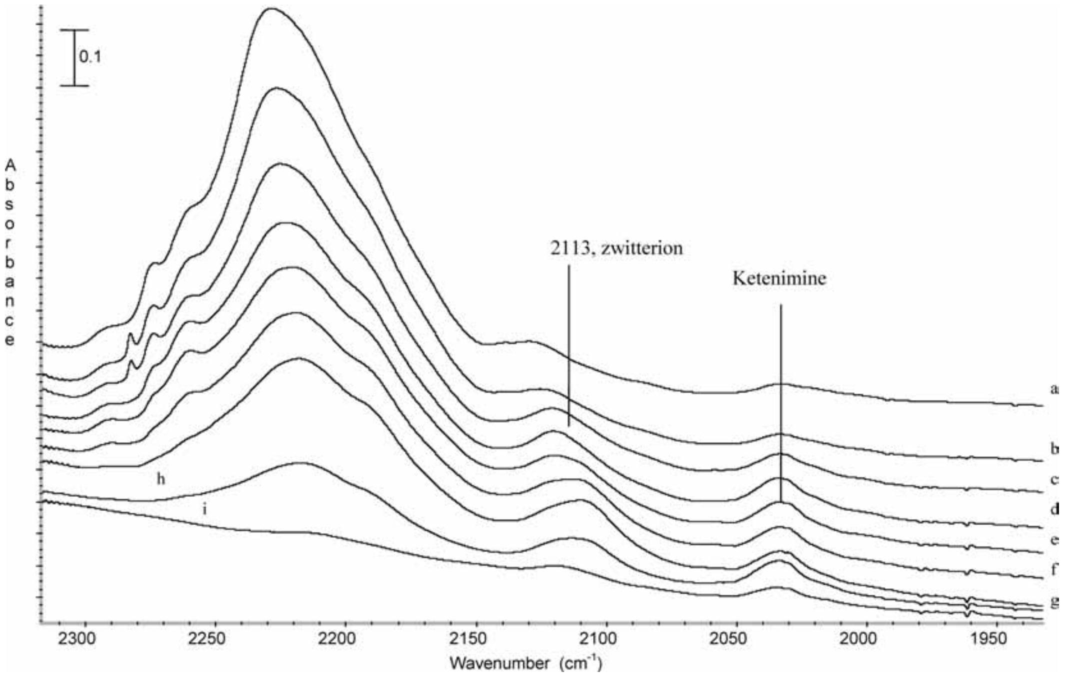

Figure 5. 3-Pyridyliminopropadienone (**4d**) from **1d** with DMA deposited at 50 K, recorded at (a) 50 K, (b) 80 K, (c) 100 K, (d) 120 K, (e) 130 K, (f) 140 K, (g) 150 K, (h) 160 K, and (i) 180 K.

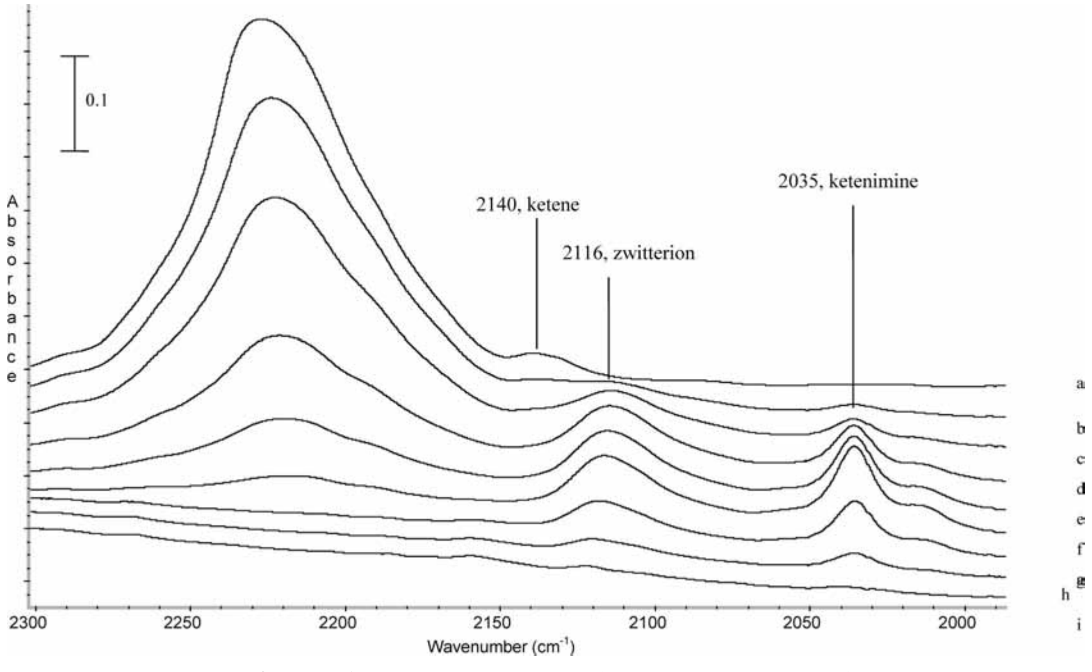

Figure 6. 3-Pyridyliminopropadienone (**4d**) from **1d** with DEA deposited at 50 K, then recorded at (a) 50 K, (b) 90 K, (c) 100 K, (d) 110 K, (e) 120 K, (f) 130 K, (g) 140 K, (h) 150 K, and (i) 160 K.

growing till 130 K and then began to decrease. The results from the TMA experiment (vide supra) suggest that the 2113 cm^{-1} species is a zwitterion analogous to **5** or **6** (**11** or **12**, Scheme 4, Table 1). The 2039 cm^{-1} band continued to grow till 140 K and is ascribed to the formation of ketenimine **9b** in the matrix. When **4b** was deposited with DMA, this ketenimine band was weakly present already in the deposition spectrum at 50 K, indicating the formation of ketenimine **7b** (minor) along with ketene **8b** (major) in the gas-phase reaction (see Scheme 3). This ketenimine band grew strongly from 110−120 K onward and indicates the preferential formation of ketenimine **9b** in the matrix.

Upon deposition of 3-pyridyliminopropadienone **4d** with DMA or DEA, the appearance of weak bands at ca. 2140 and 2035 cm^{-1} indicates the formation of small amounts of both ketene and ketenimine in a gas-phase reaction (Figures 5 and 6). In the deposition with DMA, the ketenimine band at 2034 cm^{-1} was observed to grow from ca. 100 K as a result of a reaction of DMA with 3-pyridyliminopropadienone **4d** (2226 cm^{-1}) in the matrix (Figure 5). The band of 3-pyridyliminopropadienone decreased as the 2034 cm^{-1} band increased, and the latter is assigned to ketenimine **7d**. A similar reaction was observed with DEA, and the resulting ketenimine **9d** had a band at 2035 cm^{-1} when **4d** was generated from the Meldrum's acid

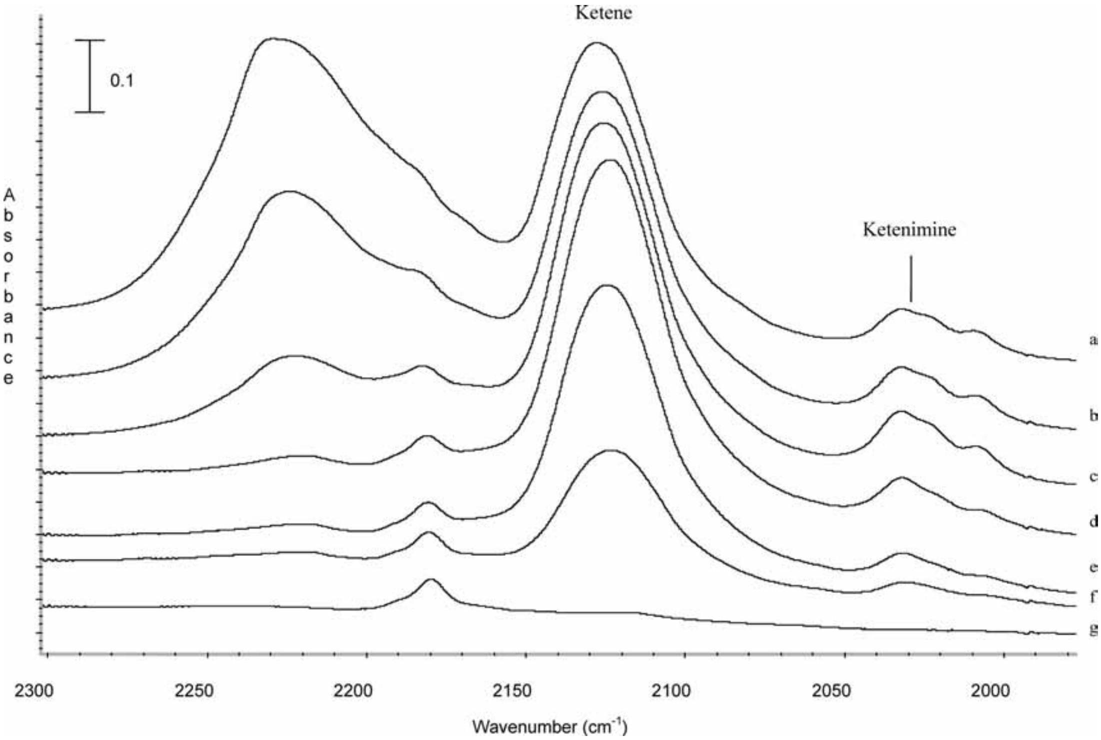

Figure 7. 2-Pyridyliminopropadienone (**4c**) from **3** with DMA deposited at 50 K, recorded at (a) 50 K, (b) 80 K, (c) 100 K, (d) 130 K, (e) 140 K, (f) 150 K, and (g) 180 K.

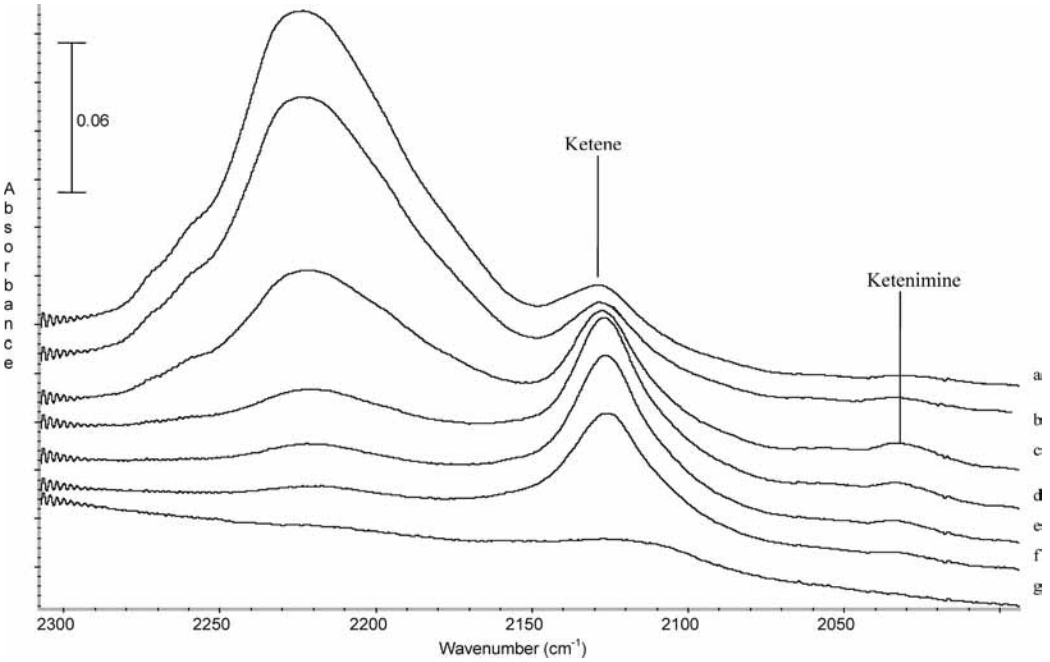

Figure 8. 4-Pyridyliminopropadienone (**4e**) from **1e** with DMA deposited at 50 K, recorded at (a) 50 K, (b) 80 K, (c) 100 K, (d) 130 K, (e) 140 K, (f) 150 K, and (g) 180 K.

derivative **1d** (Figure 6) and at 2028 cm^{-1} when **4d** was generated from the isoxazolopyrimidinone **2d**. In Figure 6, a band is seen to grow at 2116 cm^{-1} from 90 K onward. This band is in the range of the zwitterions **5** and **6** (**11** and **12**, Scheme 4). At 110 K, it reached maximum intensity and then began to decrease. At the same time, the ketenimine band at 2035 cm^{-1}, assigned to **9d**, continued to grow till 120 K.

2-Pyridyliminopropadienone **4c** was codeposited with DMA at 50 K (Figure 7) and characterized by a strong band at 2231 cm^{-1}. Interestingly, an intense band at 2124 cm^{-1} corresponding to the ketene **8c** was also present. This is ascribed to a gas-phase reaction between 2-pyridyliminopropadienone and DMA, and a growth of this band was observed during the annealing process until 110 K. In addition, a weak band at 2028 cm^{-1} was also growing between 80 and 100 K and corresponds to ketenimine **7c**. The intensity of **4c** was seen to decrease at the same time. The fact that both ketene and ketenimine products are observable indicates that the reactivities of the C═O and

C=N subunits in **4c** are of the same order of magnitude. The normal reactivity[5] should lead to preferential reaction with the C=O carbon and hence formation of ketenimine **7**. The electron-withdrawing 2-pyridyl group may increase the electrophilicity of the N=C carbon, causing more of the abnormal reaction product to form, as has been seen in the preparative experiments.[19]

Codeposition of 4-pyridyliminopropadienone **4e** (from **1e**) with DMA at 50 K resulted in a strong band at 2223 cm^{-1}, due to **4e,** and a weaker band at 2127 cm^{-1} (Figure 8). Analogously to the case of 2-pyridyliminopropadienone, the weak band at 2127 cm^{-1} grew during the annealing process, and it is ascribed to the ketene **8e**. At 100 K, a ketenimine band at 2033 cm^{-1} was also observed. These observations again indicate that the electron withdrawing effect of the 4-pyridyl group may activate the N=C carbon toward nucleophilic attack.

When **4e** was deposited with DEA, a large structured band at 2127 cm^{-1} began to grow around 110 K (see Supporting Information). This is in the ketene region and is ascribed to the formation of **10e**. A band at 2113 cm^{-1} was also observed around 110 K and disappeared totally at 120 K, whereas the 2127 cm^{-1} band stayed till 160 K. As described above, the band at 2113 cm^{-1} corresponds to a zwitterionic intermediate (**11** or **12**, Scheme 4). At 110 K, another band appeared at 2036 cm^{-1}, which corresponds to the formation of ketenimine **9e**. The main observed and calculated bands are correlated in Tables 2 and 3. Importantly, iminopropadienone **4e** appears to form ketenes (**8e** and **10e**) much more readily than ketenimines (**7e** and **9e**).

Close inspection of the data presented in Table 1 indicates that the intermediates formed in the reactions with secondary amines derived from the addition to the C=O end of the molecule, in accordance with the findings for the TMA addition.

Conclusion

Preparative scale experiments have revealed that the iminopropadienones RN=C=C=C=O usually react with nucleophiles and bisnucleophiles, first, on the more electrophilic C=O carbon and, second, on the C=N carbon. However, exceptions were noted for the 2,6-difluorophenyl derivative **4b** and the 2-pyridyl derivatives **4c**, where significant amounts of additional products derived from the alternative mode of attack (first C=N, second C=O) were isolated and characterized.[5,18]

The present experiments provide direct evidence for nucleophilic attack on both the C=O and C=N moieties in iminopropadienones. The iminopropadienones **4a**−**e** isolated at low temperatures in amine matrices react with amines (TMA, DMA, DEA) at 70−90 K to form zwitterions **5** and/or **6** and **11** and/or **12** observable in the IR spectra at ca. 2110−2117 cm^{-1}. A clear distinction between the two types of zwitterion cannot be made, but the data are in good agreement with calculations for preferred attack on the C=O bonds to form ketenimine-type zwitterions. In the reactions with secondary amines (DMA and DEA), the formation of imidoylketenes **8**(**10**) predominates in the gas-phase reactions, except in the case of **4a**, whereas the formation of oxoketenimines **7**(**9**) predominates in the matrix reactions. Notably, the 2,6-difluorophenyl, the 2-pyridyl, and the 4-pyridyl substituent in **4b**, **4c**, and **4e**, respectively, appear to activate the C=N moieties toward nucleophilic attack, resulting in the preferred formation of ketenes **8**(**10**) in the reactions with secondary amines in low temperature matrices.[19]

The formation of a zwitterion analogous to **5** or **6** (cf. Scheme 2) was also observed in the reaction of **4b** with pyridine. In some cases (**4b**, **4d**, and **4e**), zwitterion intermediates **11** and/or **12** (2113−2116 cm^{-1}) were also observed in the reactions with the secondary amines, particularly DEA. These species disappeared again at 110−120 K, whereas bands due to ketenimines **7** (**9**) continued to grow. Thus, zwitterions **11** and **12** are assumed to be intermediates in the formation of ketenimines **7**(**9**) and ketenes **8**(**10**) as indicated in Scheme 4.

Detailed computational studies relating to these reaction pathways are described in a separate paper.[19]

Acknowledgment. This work was supported by the Australian Research Council Linkage-International and Discovery grants, the APAC national computational facility Merit Allocation Scheme, and the University of Queensland Centre for Computational Molecular Science.

Supporting Information Available: Preparative experimental details and compound characterization. IR spectra of the products of all the FVT reactions (full range (400−4000 cm^{-1}) as well as the 1900−2400 cm^{-1} ranges). Cartesian coordinates and relevant frequencies for all calculated compounds. This material is available free of charge via the Internet at http://pubs.acs.org.

References and Notes

(1) Sessouma, B.; Couturier-Tamburelli, I.; Monnier, M.; Wong, M. W.; Wentrup, C.; Aycard, J. P. *J. Phys. Chem. A* **2002**, *106*, 4489.

(2) For the formation of zwitterions in reactions of ketenes, see (a) Tidwell, T. T. *Ketenes*; John Willey & sons, Inc.: New York, 1995. (b) Qiao, G. G.; Andraos, J.; Wentrup, C. *J. Am. Chem. Soc.* **1996**, *118*, 5634. (c) Visser, P.; Zuhse, R.; Wong, M. W.; Wentrup, C. *J. Am. Chem. Soc.* **1996**, *118*, 12598. (d) Kollenz, G.; Holzer, S.; Dalvi, T. S.; Kappe, C. O.; Fabian, W. M. F.; Sterk, H.; Wong, M. W.; Wentrup, C. *Eur. J. Org. Chem.* **2001**, 1315.

(3) (a) Mosandl, T.; Kappe, C. O.; Flammang, R.; Wentrup, C. *J. Chem. Soc., Chem. Commun.* **1992**, 1571. (b) Mosandl, T.; Stadtmüller, S.; Wong, M. W.; Wentrup, C. *J. Phys. Chem.* **1994**, *98*, 1080. (c) Wentrup, C.; Ramana Rao, V. V.; Frank, W.; Fulloon, B. E.; Moloney, D. W. J.; Mosandl, T. *J. Org. Chem.* **1999**, *64*, 3608. (d) Plüg, C.; Frank, W.; Wentrup, C. *J. Chem. Soc., Perkin Trans. 2* **1999**, 1087. (e) Bibas, H.; Moloney, D. W. J.; Neumann, R.; Shtaiwi, M.; Bernhardt, P. V.; Wentrup, C. *J. Org. Chem.* **2002**, *67*, 2619.

(4) Koch, R.; Bruhn, T.; Veedu, R. N.; Wentrup, C. *THEOCHEM* **2004**, *686*, 31.

(5) Shtaiwi, M.; Wentrup, C. *J. Org. Chem.* **2002**, *67*, 8558.

(6) (a) Taylor, E. C.; Garcia, E. J. *J. Org. Chem.* **1964**, *29*, 2116. (b) Rajagopalan, P.; Talaty, C. N. *Tetrahedron* **1967**, *23*, 3541.

(7) Coda, A. C.; Tacconi, G. *Gazz. Chim. Ital.* **1984**, *114*, 131.

(8) Frisch, M. J.; Trucks, G. W.; Schlegel, H. B.; Scuseria, G. E.; Robb, M. A.; Cheeseman, J. R.; Montgomery, J. A., Jr.; Vreven, T.; Kudin, K. N.; Burant, J. C.; Millam, J. M.; Iyengar, S. S.; Tomasi, J.; Barone, V.; Mennucci, B.; Cossi, M.; Scalmani, G.; Rega, N.; Petersson, G. A.; Nakatsuji, H.; Hada, M.; Ehara, M.; Toyota, K.; Fukuda, R.; Hasegawa, J.; Ishida, M.; Nakajima, T.; Honda, Y.; Kitao, O.; Nakai, H.; Klene, M.; Li, X.; Knox, J. E.; Hratchian, H. P.; Cross, J. B.; Bakken, V.; Adamo, C.; Jaramillo, J.; Gomperts, R.; Stratmann, R. E.; Yazyev, O.; Austin, A. J.; Cammi, R.; Pomelli, C.; Ochterski, J. W.; Ayala, P. Y.; Morokuma, K.; Voth, G. A.; Salvador, P.; Dannenberg, J. J.; Zakrzewski, V. G.; Dapprich, S.; Daniels, A. D.; Strain, M. C.; Farkas, O.; Malick, D. K.; Rabuck, A. D.; Raghavachari, K.; Foresman, J. B.; Ortiz, J. V.; Cui, Q.; Baboul, A. G.; Clifford, S.; Cioslowski, J.; Stefanov, B. B.; Liu, G.; Liashenko, A.; Piskorz, P.; Komaromi, I.; Martin, R. L.; Fox, D. J.; Keith, T.; Al-Laham, M. A.; Peng, C. Y.; Nanayakkara, A.; Challacombe, M.; Gill, P. M. W.; Johnson, B.; Chen, W.; Wong, M. W.; Gonzalez, C.; Pople, J. A. *Gaussian 03*, revision B.05; Gaussian, Inc.: Wallingford, CT, 2004.

(9) (a) Becke, A. *J. Chem. Phys.* **1993**, *98*, 5648. (b) Lee, C.; Yang, W.; Parr, R. G. *Phys. Rev. Sect B* **1988**, *37*, 785.

(10) (a) Hariharan, P. C.; Pople, J. A. *Theor. Chim. Acta* **1973**, *28*, 213. (b) Pietro, W. J.; Francl, M. M.; Hehre, W. J.; DeFrees, D. J.; Pople, J. A.; Binkley, J. S. *J. Am. Chem. Soc.* **1982**, *104*, 5039.

(11) (a) Cancès, M. T.; Mennucci, B.; Tomasi, J. *J. Chem. Phys.* **1997**, *107*, 3032. (b) Cossi, M.; Barone, V.; Mennucci, B.; Tomasi, J. *Chem. Phys. Lett.* **1998**, *286*, 253. (c) Mennucci, B.; Tomasi, J. *J. Chem. Phys.* **1997**, *106*, 5151.

(12) (a) Plüg, C.; Wallfisch, B.; Andersen, H. G.; Bernhardt, P. V.; Baker, L.-J.; Clark, G.; Wong, M. W.; Wentrup, C. *J. Chem. Soc., Perkin Trans. 2* **2000**, 2096. (b) Finnerty, J.; Mitschke, U.; Wentrup, C. *J. Org. Chem.* **2002**, *67*, 1084. (c) Finnerty, J. J.; Wentrup, C. *J. Org. Chem.* **2004**, *69*, 1909. (d) Finnerty, J.; Wentrup, C. *J. Org. Chem.* **2005**, *70*, 3795.

(13) (a) Wong, M. W. *Chem. Phys. Lett.* **1996**, *256*, 391. (b) Scott, A. P.; Radom, L. *J. Phys. Chem.* **1996**, *100*, 16502.

(14) Bossa, J. B.; Borget, F.; Duvernay, F.; Theulé, P.; Chiavassa, T. *J. Phys. Chem. A,* **2008**, *112*, 5113.

(15) Raunier, S.; Chiavassa, T.; Marinelli, F.; Allouche, A.; Aycard, J. P. *Chem. Phys. Lett.* **2003**, *368*, 594.

(16) Raunier, S.; Chiavassa, T.; Marinelli, F.; Allouche, A.; Aycard, J. P. *J. Phys. Chem. A* **2003**, *107*, 9335.

(17) Couturier-Tamburelli, I.; Aycard, J. P.; Wong, M. W.; Wentrup, C. *J. Phys. Chem. A* **2000**, *104*, 3466.

(18) Andersen, H. G.; Mitschke, U.; Wentrup, C. *J. Chem. Soc., Perkin Trans. 2* **2001**, 602–607.

(19) Koch, R.; Finnerty, J. J.; Bruhn, T.; Borget, F.; Wentrup, C. *J. Phys. Chem. A* **2008**, *112*, 8999–9004.

JP803351Q